Reaction Characteristics of the In-15Pb-5Ag Solder with a Au/Ni/Cu Pad and Their Effects on Mechanical Properties

JONG-HYUN LEE,[1] YONG-SEONG EOM,[1] KWANG-SEONG CHOI,[1] BYUNG-SEOK CHOI,[1] HO-GYEONG YOON,[1] JONG-TAE MOON,[1] and YONG-SEOG KIM[2,3]

1.—Integrated Optical Module Team, ETRI, Daejeon, Korea. 2.—Department of Materials Science and Engineering, Hong Ik University, Seoul, Korea. 3.—yskim@wow.honghik.ac.kr

Reaction characteristics of the In-15Pb-5Ag (wt.%) solder with a Au/Ni/Cu pad during reflow soldering and aging treatment were examined. Interfacial reaction during reflow resulted in either an $AuIn_2$ or $Ni_{28}In_{72}$ layer, depending on reflow time. The $AuIn_2$ layer became thinner and disappeared from the interface, and only the $Ni_{28}In_{72}$ layer grew with the progress of aging treatment at 130°C. Based on those observations, the dissolution rate of the Au top layer was estimated, and the behavior of the $AuIn_2$ layer during reflow and aging treatment was discussed. In addition, peak shear load and fracture energy of the solder bump were measured as a function of reflow time and aging treatment. The results were compared with those measured with the Sn-37Pb solder bump.

Key words: In-15Pb-5Ag solder, reflow, Au dissolution, aging, Au embrittlement

INTRODUCTION

Traditionally, Au/Ni/Cu under bump metallurgy (UBM) is frequently used in microelectronic packages for its excellent solderability and reliability. The Au top layer is to prevent oxidation and corrosion of the UBM, and the Ni layer limits extensive reaction between the solder and UBM layers.[1,2] Use of a thick Au layer for Sn-37Pb solder joints, however, has resulted in a dramatic reduction in ductility of the solder interconnection, causing so-called Au embrittlement.[3–7] In the interconnection, rapid redeposition of the Au-containing ternary intermetallic layer at the solder/UBM interface during aging treatment was observed.[7–12] The inherent lattice strain and volume change upon the formation of the ternary compound layer have been identified as the main causes of the embrittlement.[12] This type of embrittlement was observed to occur when Au content in the solder exceeds its solubility limit, 0.3 wt.%.[7,8,10,12] The embrittlement was abated significantly by alloying the solder with Cu or Ni.[7,11,14]

(Received August 19, 2003; accepted December 17, 2003)

Recently, In-based solders are being used for solder interconnections in microwave devices.[13] Among In-based solders, In-15Pb-5Ag (wt.%) solder is preferred because it has a higher strength than pure indium and a smaller thermal expansion coefficient, $\sim 10 \times 10^{-6}$/°C. In this study, the possibility of Au embrittlement of In-15Pb-5Ag solder interconnections with the Au/Ni UBM layer was examined. The effects of reflow and aging time on the microstructure at the solder/UBM interface and mechanical properties of the solder bump on the UBM were studied. These characteristics were compared with those of the Sn-37Pb solder.

EXPERIMENTAL PROCEDURES

Solder balls of In-15Pb-5Ag (Indium Corporation of America, Utica, NY) and Sn-37Pb (Alpha Metals, New Jersey, USA) compositions were placed manually onto UBM pads formed on a substrate of bismaleimide-triazine (BT) resin. The UBM pad consisted of Au (0.5 μm)/Ni (5 μm)/Cu layers. The diameter of the solder balls used was 760 μm and that of the pads was 600 μm. For reflow soldering, the solder balls and pads were coated with rosin mildly activated flux and heated on a hot plate 40°C higher

than its liquidus temperature. The liquidus temperature of In-15Pb-5Ag solder is 154°C and that of Sn-37Pb is 183°C. The reflow time for the In-15Pb-5Ag solder was varied from 1 min to 5 min. For the Sn-37Pb solder, the reflow time was fixed to 1 min. After the reflow soldering, the samples were aged at 130°C up to 500 h.

Mechanical properties of the solder bump were evaluated using a ball-shear tester (multifunction bond tester, model: DAGE-4000, Dage Precision Industries, Fremont, CA). In the test, the peak shear load was measured, and fracture energy of the solder bump was calculated by integrating the load-displacement curve. For each condition, five samples were tested, and their values were averaged. Microstructures and fractured surfaces of solder bumps after the ball-shear test were examined using a scanning electron microscope (SEM)/backscattered electron image (BEI). Chemical compositions of the phases formed at the solder/UBM interface were evaluated using a SEM/energy dispersive spectroscope (EDS).

RESULTS AND DISCUSSION

The SEM/BEI micrographs of the In-15Pb-5Ag solder/UBM interface at various reflow times are shown in Fig. 1. With the sample reflowed for 1 min (Fig. 1a and b), a continuous layer formed at the solder/UBM interface. The EDS analysis of the layer indicated that the contents of Au and In are similar to each other. Observation of the layer at a higher magnification (Fig. 1b) revealed that it consisted of two different layers: an Au-rich layer (region A in the figure) and an In-rich layer (region B in the figure). A previous study[15] reported that the layers are the Au-In solid solution (A layer) and $AuIn_2$ phase (B layer). As the reflow time increased to 3 min, the thickness of the composite layer became thinner and discontinuous, as shown in Fig. 1c and d. As noted in the micrographs, the discontinuous layer consisted of a single phase. When the phase was analyzed using SEM/EDS, the Au content was 31–36 at.%, and the In content was 64–69 at.%, suggesting that it is the $AuIn_2$ phase. At the regions where the $AuNi_2$ layer was discontinuous to expose the Ni layer to the molten solder, a thin layer of In-Ni intermetallic formed, as shown in Fig. 1d. As the reflow time increased further to 5 min, the In-Ni intermetallic layer was observed to grow, and the $AuIn_2$ phase disappeared completely from the solder/UBM interface (Fig. 1e and f).

The thickness of each reaction layer was measured as a function of reflow time (Fig. 2). The thicknesses of the Au-rich solid solution and $AuIn_2$ layers were noted to decrease with reflow time and could not be

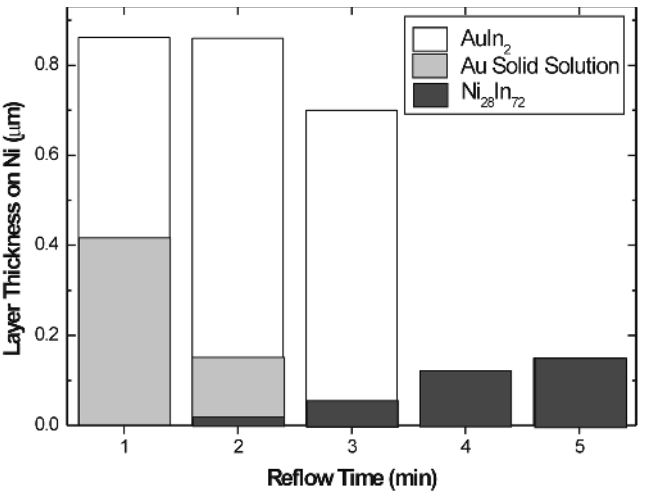

Fig. 2. Changes in type and thickness of the intermetallics formed on the Ni pad with reflow time.

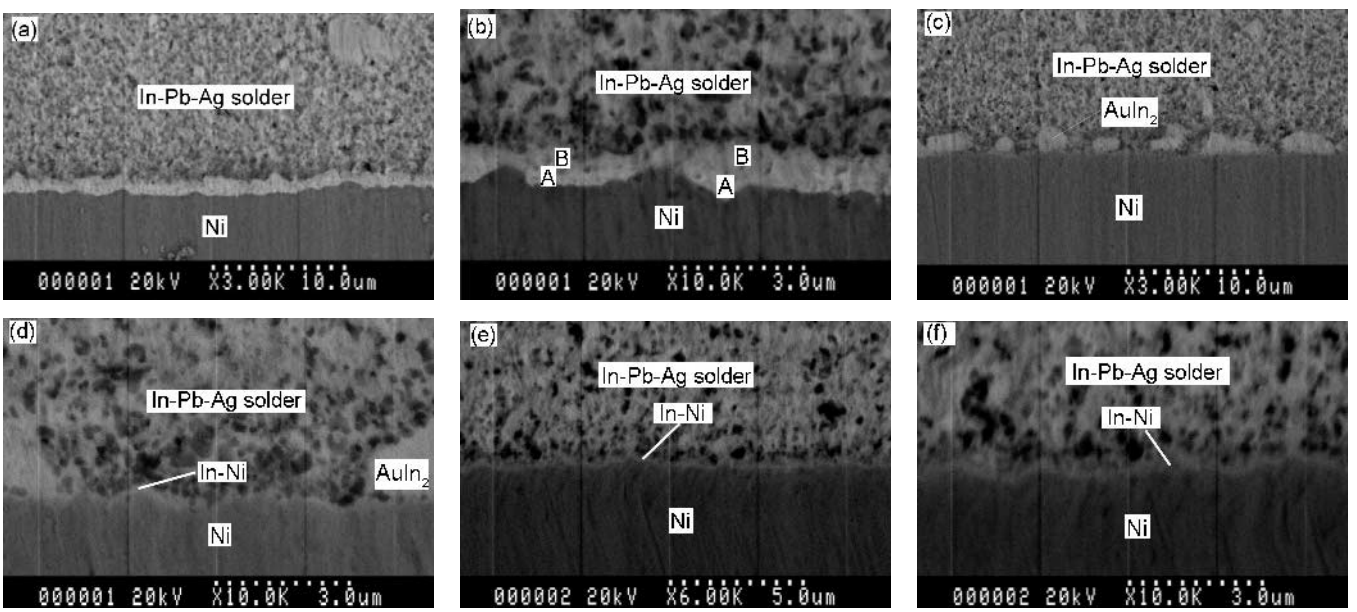

Fig. 1. SEM/BEI micrographs of the In-15Pb-5Ag/Au/Ni pad interface after reflow for different times: (a) and (b) 1 min, (c) and (d) 3 min, and (e) and (f) 5 min. The magnification of the right micrographs are larger that those on the left.

observed from the interface after 4 min of reflow. The fact that the Au-rich layer survived for 4 min of reflow indicates a very slow dissolution rate of the Au layer into the In-15Pb-5Ag solder compared to that into the Sn-37Pb solder. In previous studies, the Au layer was dissolved into molten Sn-37Pb solder within 10 sec of reflow time.[4,16] Based on this observation, the dissolution rate was estimated to be on the order of 2×10^{-3} μm/sec, significantly slower than that into Sn-37Pb solder, ~1.3 μm/sec.[4]

The disappearance of the $AuIn_2$ phase at extended reflow times might be caused by several phenomena. One is the slow dissolution rate of the Au top layer into the solder. This slower dissolution rate of the Au top layer into the In-15Pb-5Ag solder is expected to set up a temporary equilibrium[17] between the Au layer and molten solder, as long as the Au-rich layer survives on the UBM layer. The $AuIn_2$ phase, therefore, is believed to be a metastable phase formed by temporary equilibrium. As the Au layer is consumed by the reaction as well as dissolution into the solder, the phase should become unstable. If the Au content in the solder is less than its solubility, the phase should dissolve into the solder. Assuming all the Au top UBM layer dissolved into the solder, the Au content in the solder was estimated to be ~0.15 wt.% (0.1 at.%), which is much lower than its solubility in pure In, ~1 wt.% (0.5 at.%), at the reflow temperature.[18]

The other possibility of the $AuIn_2$ phase disappearance from the interface is gravity segregation of the phase by density difference. In the Sn-37Pb solder matrix, Cu_6Sn_5 precipitates were observed to segregate during reflow because of the density difference between the matrix and the precipitate.[19] The density of $AuIn_2$, estimated from its lattice constant and crystal structure, was 10.45 g/cm^3,[20] and that of In-15Pb-5Ag was 7.85 g/cm^3.[21] The heavier precipitates should segregate at the interface, rather than disappearing from the interface as observed in actual experiments.

The In-Ni intermetallic layer, on the other hand, started to form after 2 min of reflow and continued to grow with reflow time. The time exponent of the layer was estimated to be ~0.5. This result suggests that the growth might be controlled by the diffusion of reacting species through the product layer.

Figure 3 shows SEM/BEI micrographs of the samples aged for 300 h at 130°C. Reflow times for the samples were 1 min and 5 min, respectively. With the sample prepared by reflow for 1 min, a semicontinuous layer of the $AuIn_2$ phase was formed at the interface. Some part of the $AuIn_2$ layer became partially spheroidized, and a thick Ni-In intermetallic layer was formed between the $AuIn_2$ and Ni layers by the aging treatment. The thickness of the Ni-In intermetallic layer was approximately 2 μm, and its chemical compositions determined using EDS was closed to the $Ni_{28}In_{72}$ phase, as reported previously.[22] The thickness of the $Ni_{28}In_{72}$ layers formed after the aging treatment, however, was independent of the reflow time. The thickness with the samples reflowed for 3 min and 5 min were almost the same, ~2 μm. The growth of the $Ni_{28}In_{72}$ layer was not affected by the presence of the Au-rich and $AuIn_2$ layers. The diffusivity of reacting species through the $AuIn_2$ layer must have been much faster than that through the $Ni_{28}In_{72}$ layer. Within the solder matrix, $AgIn_2$ precipitates coarsened significantly with aging treatment. Very fine precipitates of submicron size after reflow coarsened to 5 μm.

With the Sn-37Pb solder, a 0.4-μm-thick Ni_3Sn_4 layer formed after reflow soldering. The aging treatment of the Sn-37Pb solder at 130°C for 300 h, on the other hand, increased the thickness of the Au-Ni-Sn ternary intermetallic layer to 2.4 μm and

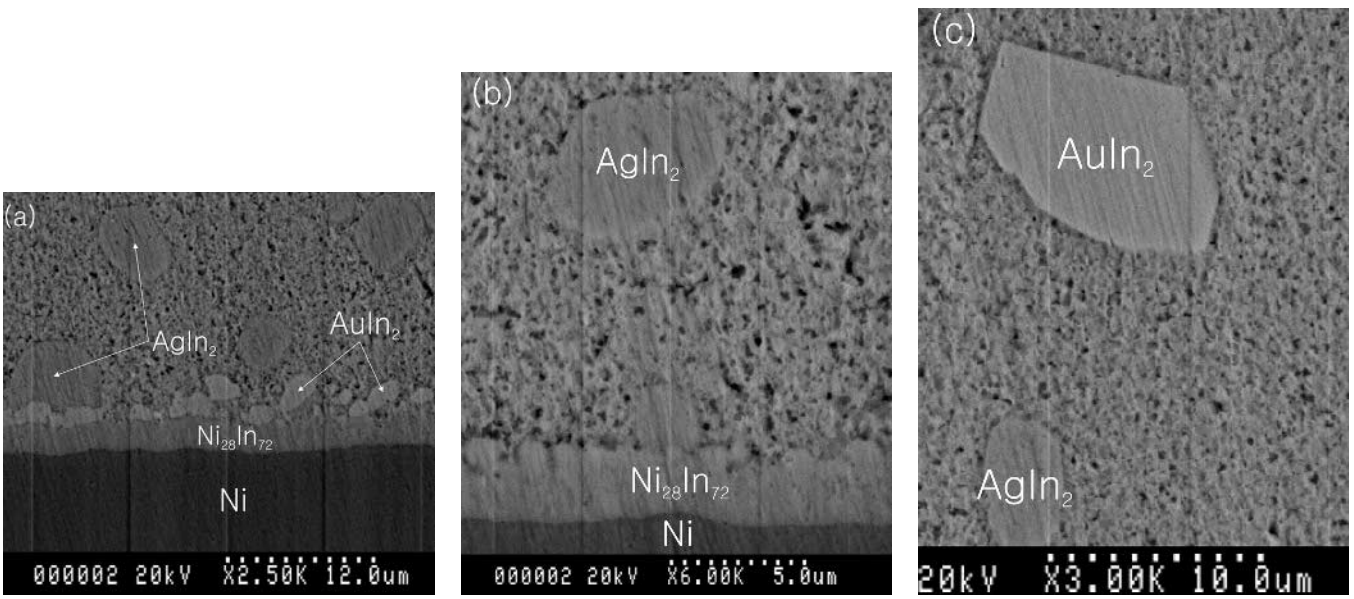

Fig. 3. SEM/BEI micrographs of the In-15Pb-5Ag/Au/Ni pad after aging treatment for 300 h at 130°C: (a) reflowed for 1 min and (b) and (c) reflowed for 5 min.

the Ni_3Sn_4 layer to 0.7 μm. The microstructure of the layer was similar to that obtained with the sample aged at 150°C, but was thinner.[7] The formation of the ternary intermetallic layer was attributed to the decomposition of $AuSn_4$ in the solder matrix, followed by formation of a more thermodynamically stable ternary compound at the interface.[8–12]

As the aging time for the In-15Pb-5Ag solder reflowed for 1 min increased to 500 h, the thickness of the $Ni_{28}In_{78}$ layer increased to ~3 μm, and the $AuIn_2$ layer almost disappeared from the interface (Fig. 4a). The Au-containing phase disappeared from the interface rather than redepositing at the interface as found for the Sn-37Pb solder matrix during the aging treatment. Gold atoms from the $AuIn_2$ phase might dissolve into the solder matrix or react with the $Ni_{28}In_{72}$ phase to form a ternary intermetallic compound at the interface. The EDS analysis of the Ni-In ($Ni_{28}In_{72}$) layer, however, revealed only a trace amount of Au in the layer. In addition, the thickness and microstructure of the interface layer were similar to that reflowed for 5 min, followed by 500 h of aging treatment (Fig. 4b). With the sample reflowed for 5 min, only the $Ni_{28}In_{72}$ layer formed after reflow soldering, and the layer was not in contact with the $AuIn_2$ phase. These results indicate that the $AuIn_2$ phase decomposes and dissolves into the solder matrix during aging.

Figure 5 shows a load-displacement curve of the ball-shear test of In-15Pb-5Ag and Sn-37Pb solder bumps under the as-reflowed condition. The gap between the stylus tip and the pad was 10 μm, and the speed of the tip was 200 μm/sec. A detailed description of ball-shear testing can be found elsewhere.[7] As noted in the figure, the maximum shear load with the In-15Pb-5Ag solder is significantly smaller than that of the Sn-37Pb solder. The lower tensile strength of In-15Pb-5Ag, 17.6 MPa, than that of Sn-37Pb solder, 51.7 MPa, should have contributed to the difference.[21] The fracture shear displacements of both solders were similar to each other. The shear displacement of the aged solder bumps, however,

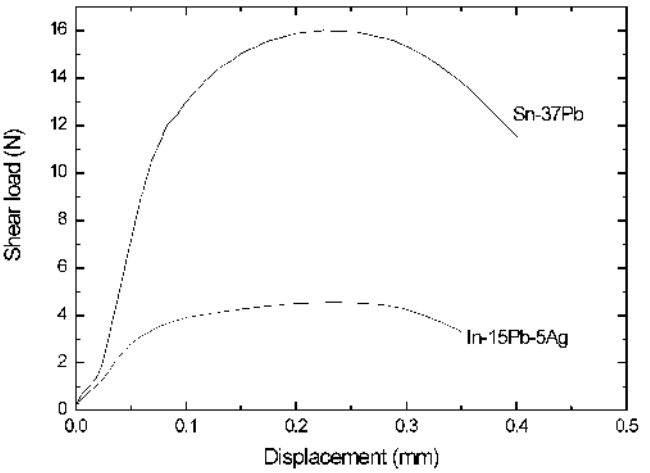

Fig. 5. Shear load-displacement curve of a solder bump in the as-reflowed condition. The reflow time was 1 min: (a) In-15Pb-5Ag and (b) Sn-37Pb solder bump.

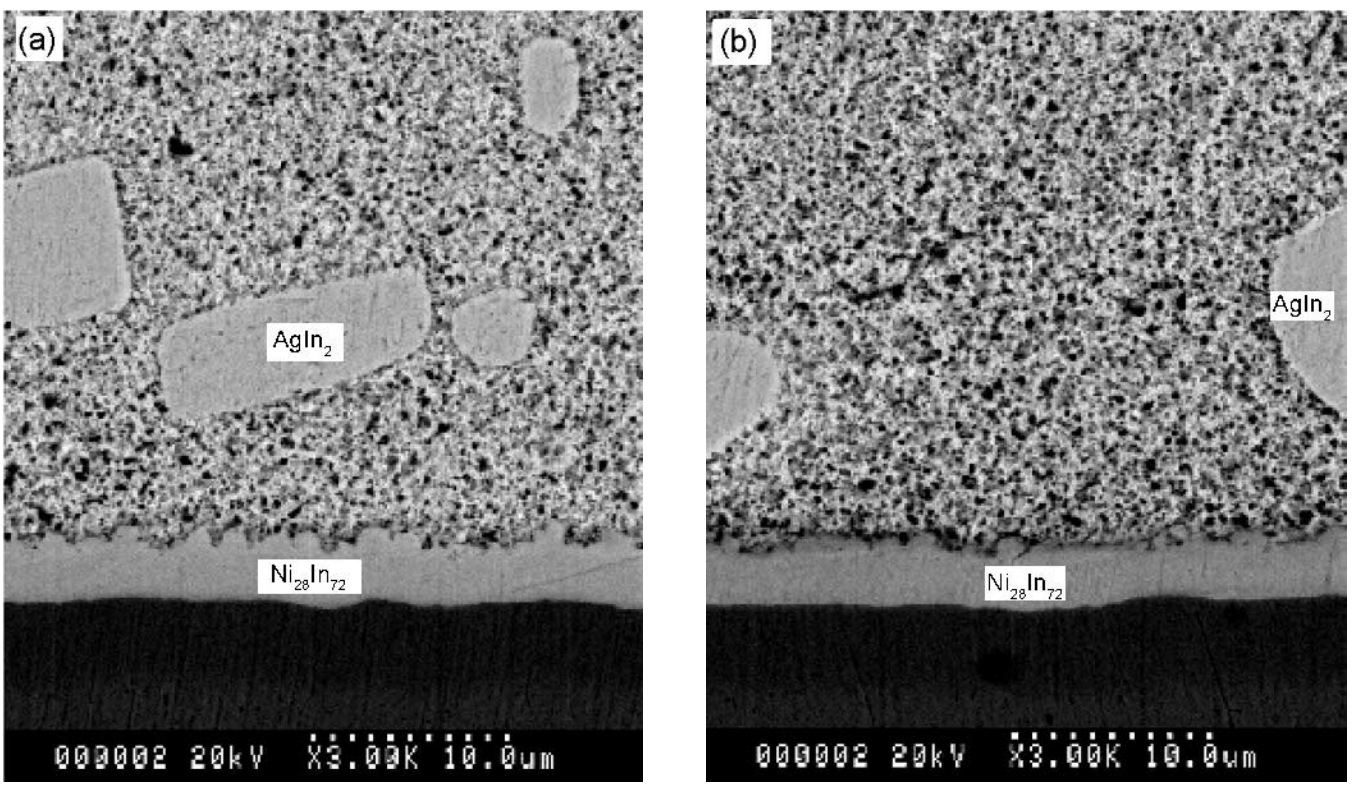

Fig. 4. SEM/BEI micrographs of the In-15Pb-5Ag/Au/Ni pad interface after aging treatment for 500 h at 130°C: (a) reflowed for 1 min and (b) and (c) reflowed for 5 min.

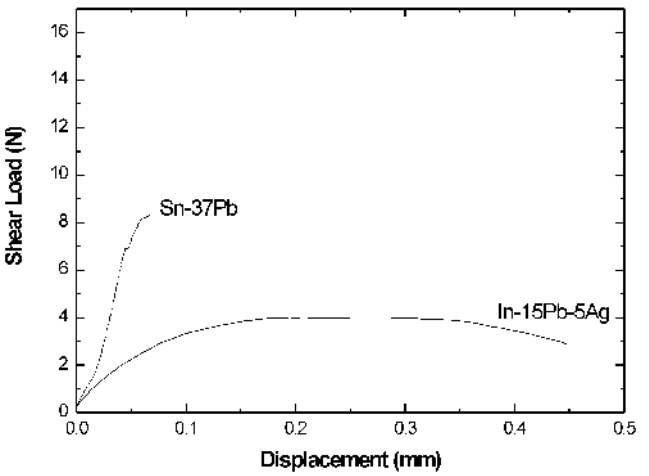

Fig. 6. Shear load-displacement curve of a solder bump after aging for 500 h at 130°C: (a) In-15Pb-5Ag and (b) Sn-37Pb solder bump.

was affected significantly, depending on the solders used (Fig. 6). The shear displacement of the In-15Pb-5Ag solder bumps increased slightly from 0.35 mm to 0.45 mm with aging treatment. The displacement with the aged Sn-37Pb solder, on the other hand, decreased from 0.4 mm to less than 0.1 mm with treatment.

The peak shear loads measured for each solder bump are summarized in Fig. 7 as a function of aging time. The peak load for the Sn-37Pb solder decreased monotonically with aging time. The decrease in peak load reflects the effects of coarsening of the solder microstructure as well as the Au embrittlement of the interface by the redeposition of Au-ternary intermetallics. The Sn-37Pb solder bump aged for 500 h fractured in a brittle manner, indicating Au embrittlement. The peak load with the In-15Pb-5Ag solder bump remained constant with reflow and aging time. All the samples fractured in a ductile manner within the solder bump.

Fracture energies estimated for each solder bump are shown in Fig. 8. The fracture energy of the solder bump during the ball-shear test was estimated by in-

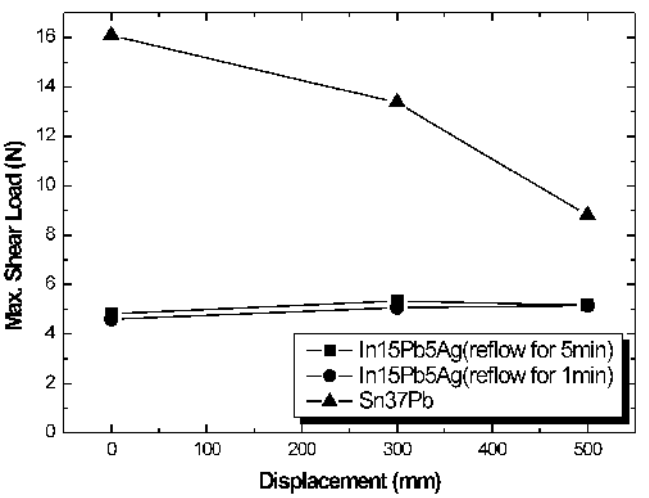

Fig. 7. Peak shear load of solder bumps as a function of aging time.

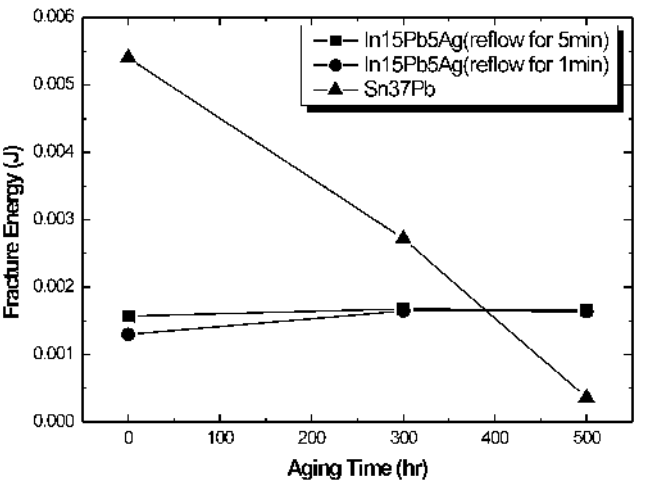

Fig. 8. Fracture energy of solder bumps as a function of aging time.

tegrating the area underneath the shear loaddisplacement curve, as shown in Fig. 5. With Sn-37Pb solder bumps, the energy decreased significantly with aging treatment. The energy of the as-reflowed bump was 0.0054 J, but that of the aged bump for 500 h at 130°C was reduced to 0.00036 J. The fracture energy decreases by a factor of 7 by the aging treatment, revealing characteristics of Au embrittlement.[4–7] The fracture energy of the In-15Pb-5Ag solder bump, however, remained constant even after aging treatment for 500 h. The absence of the Au-containing ternary compound at the solder/UBM interface and the slower growth rate of $Ni_{28}In_{72}$ might have contributed to the constant fracture energy of the solder bump. Unlike the Sn-37Pb solder, the Au-containing compound, the $AuIn_2$ phase, disappeared from the interface, effectively reducing the intermetallic layer thickness.

Figure 9 shows SEM micrographs of the fractured surface of the solder bump after ball-shear testing. In both the In-15Pb-5Ag and Sn-37Pb solder-bump, as-reflowed condition, the fracture occurred within the solder, as shown in Fig. 9a. After aging for 500 h, the fracture with the In-15Pb-5Ag solder occurred within the solder (Fig. 9b). The fracture with the Sn-37Pb solder bumps, however, occurred between Au-Ni-Sn and the Ni_3Sn_4 layer in a brittle manner, as shown in Fig. 9d. With the sample aged for 300 h, brittle fracture between the layers and ductile fracture within the solder were mixed (Fig. 9c).

CONCLUSIONS

In this study, microstructural development at the In-15Pb-5Ag solder and Au/Ni/Cu UBM interface during reflow and aging treatment was examined. At short reflow times, such as 1 min, the reaction layer consisted of the Au-rich and $AuIn_2$ reaction layers. As the reflow time increased to 5 min, the Au-rich layer dissolved into the solder matrix, and a thin layer of $Ni_{28}In_{72}$ phase was formed. The dissolution rate of the top Au layer into the molten In-15Pb-5Ag solder was estimated to be $\sim 2 \times 10^{-3}$ μm/sec, 3 orders of

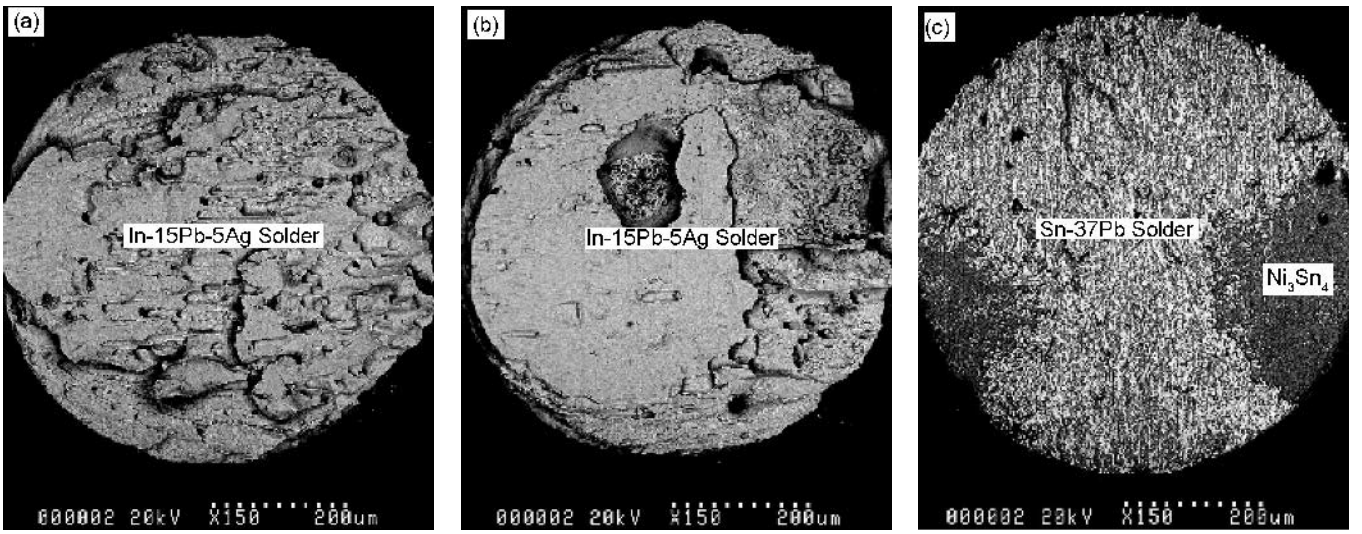

Fig. 9. SEM micrographs of a fractured surface on the pad side: (a) as-reflowed In-15Ag-5Ag solder bump, (b) In-15Ag-5Ag solder bump after aging for 500 h, (c) Sn-37Pb solder bump after aging for 300 h, and (d) Sn-37Pb solder bump after aging for 500 h. The aging temperature was 130°C.

magnitude slower than that into Sn-based solders. During aging treatment, the $AuIn_2$ layer formed during the reflow step disappeared from the interface, effectively reducing the thickness of the intermetallic layer. Fracture energy, estimated by integrating the shear load-displacement curve, remained almost the same with aging treatment, indicating the In-15Pb-5Ag solder is immune to Au embrittlement.

ACKNOWLEDGEMENTS

The authors thank Professors K.W. Paik and H.J. Kim from KAIST for conducting the ball-shear testing for this study. One of the authors (YSK) appreciates the financial support from KOSEF (Contract No. 1999-2-391-007-4).

REFERENCES

1. M. Pecht, *Integrated Circuit, Hybrid, and Multichip Module Package Design Guidelines: A Focus on Reliability* (New York: John Wiley & Sons, Inc., 1994), pp. 183–224.
2. T.-Y. Pan, H.D. Blair, J.M. Nicholson, and S.-W. Oh, *Advances in Electronic Packaging*, ed. E. Suhir, M. Shiraton, and Y.C. Lee (New York: ASME, 1997), pp. 1347–1355.
3. Z. Mei, M. Kaufmaan, A. Eslambolchi, and P. Johnson, *Proc. 48th Electronic Components and Technology Conf.* (Piscataway, NJ: IEEE, 1998), pp. 952–961.
4. A. Zribi, R.R. Chromik, R. Presthus, J. Clum, K. Teed, L. Zavalij, J. DeVita, J. Tova, and E.J. Cotts, *Proc. 49th Electronic Components and Technology Conf.* (Piscataway, NJ: IEEE, 1999), pp. 451–457.
5. S.C. Hung, P.J. Zheng, S.C. Lee, and J.J. Lee, *IEEE/CPMT Int. Electronic Manufacturing Technology Symp.* (Piscataway, NJ: IEEE, 1999), pp. 7–15.
6. R. Erich, R.J. Coyle, G.M. Wenger, and A. Primavera, *IEEE/CPMT Int. Electronic Manufacturing Technology Symp.* (Piscataway, NJ: IEEE, 1999), pp. 16–22.
7. J.-H. Lee, J.-H. Park, D.-H. Shin, Y.-H. Lee, and Y.-S. Kim, *J. Electron. Mater.* 30, 1138 (2001).
8. A.M. Minor and J.W. Morris, Jr., *Metall. Trans. A* 31A, 798 (2000).
9. A. Zribi et al., *IEEE Trans. Comp. Packaging Technol.* 23, 383 (2000).
10. A.M. Minor and J.W. Morris, Jr., *J. Electron. Mater.* 29, 1170 (2000).
11. C.E. Ho, R. Zheng, G.L. Luo, A.H. Lin, and C.R. Kao, *J. Electron. Mater.* 29, 1175 (2000).
12. H.G. Song, J.P. Ahn, A.M. Minor, and J.W. Morris, Jr., *J. Electron. Mater.* 30, 409 (2001).
13. T.S. Laverghetta, *Microwave Materials and Fabrication Techniques*, 3rd ed. (Dedham, MA: Artech House Inc., 2000), pp. 116–126.
14. K. Uenishi, T. Saeki, Y. Kohara, K.F. Kobayashi, I. Shoji, M. Nishiura, and M. Yamamoto, *Mater. Trans.* 42, 756 (2001).
15. K.J. Puttlitz, *IEEE Trans. Comp. Hybrid Manufacturing Technol.* 13, 647 (1990).
16. C.E. Ho, Y.M. Chen, and C.R. Kao, *J. Electron. Mater.* 28, 1231 (1999).
17. W.K. Choi and H.M. Lee, *J. Electron. Mater.* 29, 1207 (2000).
18. H. Okamoto and T.B. Massalski, *Binary Phase Diagrams*, ed. T.B. Massalski, H. Okamoto, P.R. Subramanian, and L. Kacprzak (Materials Park, OH: ASM International, 1990), p. 382.
19. J.-H. Lee, D.-J. Park, J.-N. Heo, Y.-H. Lee, D.-H. Shin, and Y.-S. Kim, *Scripta Mater.* 42, 827 (2000).
20. Y. Cubota, K. Kifune, and K. Yamamoto, *Thin Solid Films* 286, 136 (1996).
21. Technical information from Indium Corporation of America, Utica, NY.
22. C.-Y. Huang and S.-W. Chen, *J. Electron. Mater.* 31, 152 (2002).